Eur Spine J (2010) 19:1899–1906
DOI 10.1007/s00586-010-1434-6

ORIGINAL ARTICLE

The impact of preoperative magnetic resonance images on outcome of cemented vertebrae

Wei-Che Lin · Cheng-Hsien Lu · Hsiu-Ling Chen · Hung-Chen Wang · Chun-Yen Yu · Re-Wen Wu · Yu-Fan Cheng · Chun-Chung Lui

Received: 1 September 2009 / Revised: 17 April 2010 / Accepted: 2 May 2010 / Published online: 7 July 2010

Abstract Refracture of cemented vertebrae is often seen after percutaneous vertebroplasty. The purpose of this prospective study was to evaluate pre-procedural magnetic resonance images (MRI) for the prediction of further collapse and vertebral height loss after vertebroplasty. This study included 81 consecutive patients (73 women and 8 men) with osteoporotic compression fractures. MR studies were performed 1–5 days before vertebroplasty. Patients were followed to evaluate refracture for a minimum of 6 months after treatment. Cox proportional hazards model was used to evaluate relationships between clinical data, covariates on pre-procedural MRI, and the presence of cemented vertebrae refracture. The mean refracture rate was estimated with the Kaplan–Meier method. After a mean follow-up of 23.0 ± 8.2 months, 46 cemented vertebrae (57%) experienced refracture, and the mean loss of anterior vertebral height was 11.3%. The 1-year refracture rate after vertebroplasty was 7%, and rapid increased to 76% in the third year. Cox proportional analysis showed that any 1% decrease in signal intensity on T2-weighted images of the injured vertebra will increase the refracture rate by 0.74% (OR = 0.26, 95% CI 0.08–0.81, $p = 0.02$), and a 1% increase in the poorly enhanced volume ratio will increase the refracture rate by 4.3% (OR = 5.32, 95% CI 1.22–23.14, $p = 0.03$). Quantitative pre-procedural MRI appears to be useful in exploring vertebrae with poor bone marrow integrity, which effectively predicts the subsequent refracture of cemented vertebra.

Keywords Magnetic resonance imaging · Osteoporosis · Spine · Vertebral fracture · Vertebroplasty

W.-C. Lin · H.-L. Chen · C.-Y. Yu · Y.-F. Cheng · C.-C. Lui (✉)
Department of Diagnostic Radiology, Chang Gung Memorial Hospital, Kaohsiung Medical Center, Chang Gung University College of Medicine, 123 Ta-Pei Road, Niao-Sung Hsiang, Kaohsiung 83305, Taiwan
e-mail: lchung@adm.cgmh.org.tw

W.-C. Lin
Department of Biomedical Imaging and Radiological Sciences, National Yang-Ming University, Taipei, Taiwan

C.-H. Lu
Department of Neurology, Chang Gung Memorial Hospital, Kaohsiung Medical Center, Chang Gung University College of Medicine, Kaohsiung, Taiwan

H.-C. Wang
Department of Neurosurgery, Chang Gung Memorial Hospital, Kaohsiung Medical Center, Chang Gung University College of Medicine, Kaohsiung, Taiwan

R.-W. Wu
Department of Orthopedic Surgery, Chang Gung Memorial Hospital, Kaohsiung Medical Center, Chang Gung University College of Medicine, Kaohsiung, Taiwan

Introduction

Vertebroplasty, the percutaneous injection of polymethylmethacrylate into the affected vertebral body, has been proposed as a treatment for painful osteoporotic vertebral fractures [1–3]. Using percutaneous injection of bone cement, these fractures can be stabilized and the vertebrae strengthened immediately after the procedure [4]. In addition to possible rapid reduction in pain, the immediate effect is an increase in anterior vertebral height (AVH), especially in gas-containing vertebrae [5, 6]. The restoration of AVH reduces the wedge angle of the vertebra and kyphosis in patients [6]. Realignment of the spinal column and regaining height in fractured vertebra may decrease

complications and early morbidity related to compression fractures [7].

However, refracture of cemented vertebrae [8] was evident in about 60% of reported cases with a mean follow-up of 27 months [9]. Gas-containing clefts are reported to be at increased risk for subsequent fractures, and treatment of these clefts is also associated with increased rates of adjacent fractures after vertebroplasty [8–11]. Refracture may result from unfilled space left during the procedure or crushing of fragile trabeculae underneath by the cement during follow-up [9]. Both of these causes suggest impaired bone marrow integrity of the injured vertebrae.

Magnetic resonance imaging (MRI) has been useful in the evaluation of benign osteoporotic and malignant vertebral fractures and in determining the precise vertebral level which requires treatment preoperatively [8, 12, 13]. Intravertebral cleft and bone marrow edema patterns visualized pre- and post-procedure by MRI also used to monitor pain relief and cement distribution [8, 14–16]. Whether or not preoperative MRI can be used to predict further collapse of cemented vertebrae remains uncertain.

The aim of our study was to identify pre-vertebroplasty predictors of refracture in patients with acute vertebral fractures. We explored the relationship between bone marrow integrity as determined by preoperative MRI with subsequent refracture of cemented vertebrae, and the possibility of predicting the progression of collapse after a minimum of 6 months follow-up.

Materials and methods

Patient selection

The initial cohort of this prospective study comprised 115 consecutive patients (103 women, 12 men) with a mean age of 74.3 years (range 56–91). In these patients, a total of 134 vertebral bodies were treated with percutaneous vertebroplasty at a tertiary referral center. Exclusion criteria for vertebroplasty were the following: (1) obvious compromise of the spinal canal by the protruding fragments and associated neurological signs; (2) collapse of the vertebral body with a residual height <30%, making needle placement into the vertebral body difficult; (3) old/healed vertebral compression fracture with normal bone marrow intensity. All patients had back pain refractory to conservative treatment with osteoporotic compression fractures (VCF) identified on MR imaging. Patients were recruited from Department of Orthopedics, Neurosurgery, Neurology, and Rheumatology between July 2004 and June 2007. Osteoporosis was diagnosed using bone mineral density (BMD) in the spine and femoral neck as measured by dual energy X-ray absorptiometry (Hologic Delphi A, Florida, USA). Osteoporosis was defined as spinal BMD >2.5 SD below the average value in a young person, i.e. a T score of ≤ -2.5 SD. Pre-vertebroplasty radiographic evaluation of the patients included plain radiographs and MRI studies. Vertebrae with bone marrow edema were indicated for vertebroplasty. Patients with other spinal diseases that led to compression fracture, including infection or malignancy [based on abnormal laboratory examinations, or computed tomographic (CT)-guided biopsy], were excluded from this study. The patients were then randomly observed at our clinic after treatment, or on an as-needed basis. All radiographs, including those taken pre- and post-vertebroplasty, and those taken more than 6 months after the procedure, were obtained with the patient in the supine position. Patients without available radiographs were not included in the study. Patients with radiographs that were of low quality or in which the patient was malpositioned were excluded by an experienced radiologist prior to analysis. Eight patients without qualified radiographs and preoperative MRI studies were excluded from our study. To lessen the confounding effect of multiple treatments, 19 patients previously treated for more than 1 vertebral compression fracture was also excluded. Seven patients were lost to follow-up; thus, 81 patients (73 women, 8 men; mean age 74.3 years) met the study inclusion criteria. This study was approved by the Institutional Review Board of our hospital and all patients provided informed consent for the study and surgical procedure.

MRI protocol

A pre-procedure MR study of the spine was performed using a 1.5-T MRI system (Signa, Horizontal LX 8.3, GE Medical Systems, Milwaukee, WI, USA). T1-weighted images, T2-weighted images, and T1-weighted gadopentetate dimeglumine (Gd-DTPA, Omniscan, Amersham Health As, Cork, Ireland)-enhanced fat-suppression images were obtained. A quadrature detection thoracolumbar spine coil was used for T1-weighted and T2-weighted imaging. Following T1-weighted fast gradient-echo coronal localizer images, sagittal T1-weighted spin-echo [TR, 500 ms; TE, 15 ms; slice thickness, 4.0 mm; intersection gap, 0.4 mm; field of view (FOV), 30 × 30 cm; matrix size, 380 × 224] and sagittal T2-weighted fast spin-echo (TR, 4,000 ms; TE, 85 ms; slice thickness, 4.0 mm; intersection gap, 0.4 mm; FOV, 30 × 30 cm; matrix size, 380 × 224) images were acquired in all patients. Sagittal T1-weighted spin-echo imaging with fat suppression (TR, 500 ms; TE, 15 ms; slice thickness, 4.0 mm; intersection gap, 0.4 mm; FOV, 30 cm × 30 cm; matrix size, 380 × 224) was performed immediately after administration of 10 ml of Gd-DTPA. All MR studies were performed 1–5 days before vertebroplasty.

Vertebroplasty technique

All vertebroplasty procedures were performed by two radiologists (W.C.L. and C.C.L.) according to the technique described by Jensen et al. [1]. Each radiologist had more than 3 years experience in performing vertebroplasty. Patients were placed in the prone position on the examination table and the procedure performed under intravenous conscious sedation with 25 mg diazepam (Dupin, China Chemical and Pharmaceutical, Taipei, Taiwan). For pain control, codeine (15–30 mg) was administered, and if that was insufficient, meperidine (25 mg) was given intravenously. An 11-gauge bone marrow biopsy needle (Hakko Electric Machine Works Co., Nagano, Japan) was used to puncture the collapsed vertebral body through either side of the pedicles, and the needle advanced to the anterior third of the vertebral body under bi-plane fluoroscopic guidance. Bone cement was prepared by mixing the copolymer powder with the monomer polymerization liquid (OsteoBond, Zimmer, Warsaw, IN, USA). The cement was injected into the vertebral body under fluoroscopic monitoring and the procedure immediately terminated if any of the following was observed: (1) cement reaching the posterior margin of the vertebral body; (2) obvious migration of the cement to the drainage veins.

Data collection

Patients were divided into two groups, those with and those without refracture of the cemented vertebra 6 months post-procedure. Refracture was defined as more than a 1 mm decrease in AVH between that measured post-procedure and at follow-up [5]. Patient demographic data, including age, sex, body weight, height, and lumbar spine BMD, were recorded at the time of surgery. Parameters related to the selection of the vertebral body for treatment were considered, including vertebral level of the compression fracture, patterns of vertebral fractures, and gas content in the vertebra before treatment. The amount of cement injected and any leakage of cement into the disc space was evaluated on the radiographs after vertebroplasty.

Vertebrae were categorized into two groups: vertebrae at the thoracolumbar junction (from T10 to L2) and vertebrae outside the thoracolumbar junction (from T4 to T9 or L3 to L5). The presence of an intraosseous vacuum cleft containing gas in the vertebrae was recorded before treatment. Gas-containing vertebrae were characterized by a radiolucent zone in the vertebral body in the radiographs, or defined as 'bony cleft' if MRI revealed air or fluid within the vertebrae. The patterns of vertebral fractures [17] were divided into wedge deformity (gibbus) (30 of 81) and non-wedge deformity [plana deformity (41 of 81), and biconcavity deformity (10 of 81)]. The duration of follow-up was calculated at data collection.

All measurements were done using PACS imaging display software (Centricity RA1000, GE Healthcare, Taipei, Taiwan). Two radiologists (W.C.L. and H.L.C.) measured the images. The lines for measurement were stored and confirmed by another radiologist, and agreement was reached by consensus. Digital files of pre-vertebroplasty, post-vertebroplasty, and follow-up radiographs were retrieved for measurement of the height of the anterior aspects of the collapsed vertebral body, and the height of the posterior border of an adjacent normal vertebral body. The height of the anterior border of the collapsed vertebral body was measured using standard methods [6]. To correct for possible differences in magnification ratio on the radiographs acquired before and after vertebroplasty, the ratio of the height of the collapsed vertebral body at the anterior border on the lateral view to that of the posterior border of an adjacent normal vertebral body was used as a reference. Differences in AVH within 1 mm were considered unchanged [5] to avoid biases from technical factors or inappropriate measurement.

The signal intensity (SI) of the five most central slices of the sagittal MRI was analyzed by two radiologists (W.C.L. and H.L.C.). The analysis included the injured and normal vertebrae above and below the injured vertebra in T1-weighted and T2-weighted images, and in T1-weighted Gd-DTPA-enhanced fat-suppression images. The normal vertebrae without apparent height loss and normal fatty marrow intensity were selected for analysis. Regions of interest (ROIs), covering the entire vertebrae, were identified manually in the intravertebral body area carefully so as not to contain the cortex. In T1-weighted Gd-DTPA-enhanced fat-suppression images, the SI of the well-enhanced zone, the poorly enhanced zone, and the whole of the injured vertebral body were measured. The area of each ROI was summed to yield a volume in the well and poorly enhanced zone, and the whole of the injured vertebral body. The standardized T1-, T2-weighted, and enhanced T1-weighted fat-suppression SI of the injured vertebral body was obtained by dividing the SI of the injured vertebral body by the SI of the normal vertebral body. The SI ratio and volume ratio of the poorly enhanced and well-enhanced zones were calculated (Fig. 1).

Statistical analysis

Two separate statistical analyses were performed. First, the risk factors for refracture of cemented vertebra after 6-month follow-up were determined. Effects of individual variables on the presence of refracture, including age, gender, body weight, height, lumbar spine BMD, length of follow-up, vertebral level of compression fracture, gas

Fig. 1 The signal intensity (SI) ratio and volume ratio of the region of interest (ROI) was calculated as follows. The poorly enhanced rate = $a/(a + b + c)$. The well-enhanced rate = $(b + c)/(a + b + c)$

content in the vertebra, cement injected, cement leakage into disc, and parameters of MRI were analyzed by univariate Cox proportional hazards model. Second, any imbalances between the refracture and non-refracture groups in baseline prognostic variables were considered. Analyses were repeated with adjustments based on Cox proportional hazards model. We used backward selection with likelihood-ratio statistics based on the conditional parameter estimate for model selection. The mean refracture rate was estimated with the Kaplan–Meier method. A p value of <0.05 was considered significant, and corresponding 95% confidence limits were calculated with confidence interval (CI) estimation. All analyses were conducted using SAS software (1990; SAS Statistical Institute, Cary, NC, USA).

Results

Patient demographics and the comparative results of clinical features and MRI parameters between the patient groups with and without refracture are summarized in Table 1. Patients were followed after vertebroplasty for a mean of 23.0 ± 8.2 months (range 7–39). Ten (12.3%) of 81 patients were followed for 6–12 months, 33 (40.7%) were followed for 13–24 months, and 38 (47.0%) were followed for more than 24 months. Patients with and without refracture were followed for a mean of 20.9 ± 8.0 months (range 7–39) and 25.7 ± 7.9 months (range 8–39), respectively. The Kaplan–Meier estimate of the 1-year refracture rate after vertebroplasty was 7%, and rapidly increased to 76% in the third year (Fig. 2). Forty-six patients (57%) experienced AVH loss. The mean AVH loss was 11.3% (range 3.9–53.3). There were 15 (32.6%) patients with more than 20% loss of AVH, 19 (41.3%) with 10–20% loss and 12 (26.1%) with less than 10% loss.

Statistical analysis of the clinical manifestations and MRI data between the two patient groups revealed the following significant findings: gas-containing vertebra ($p = 0.022$), pattern of vertebral fracture ($p = 0.013$), standardized SI of the injured vertebra on T2-weighted image ($p = 0.009$), SI ratio of the well-enhanced zone of the injured vertebra ($p = 0.002$), and the volume ratio of the well ($p = 0.010$) and poorly enhanced zones ($p = 0.010$) of the injured vertebra. These significant univariate factors were used in the multiple-variable Cox proportional hazards regression analysis. The results revealed that any 1% decrease in standardized SI on T2-weighted images of the injured vertebra will increase the refracture rate by 0.74% [odds ratio (OR) = 0.26, 95% CI 0.08–0.81, $p = 0.02$], and a 1% increase in the poorly enhanced volume ratio will increase the refracture rate by 4.3% (OR = 5.32, 95% CI 1.22–23.14, $p = 0.03$).

Discussion

In this study, lower SI on T2-weighted images and greater volume of the poorly enhanced zone were associated with a significantly increased rate of refracture after vertebroplasty. This result indicates that preoperative MRI is useful in detecting poor bone marrow integrity of the osteoporotic injured vertebrae, and is effective in predicting subsequent vertebral collapse after percutaneous vertebroplasty. Although only 7% of cemented vertebrae experienced refracture during the first year of follow-up, rapid AVH loss was found in the second and third years after vertebroplasty. If this situation arises, therapeutic benefit can be obtained from a repeat procedure [18]. However, refracture causes deterioration of localized kyphosis, and there is risk of neuropathy. It is reasonable for surgeons to try to predict the risk of refracture before an operation.

Previous studies have shown that risk factors related to adjacent fractures include the presence of an intraosseous cleft [8, 19], low body mass index (BMI) [10, 20], shorter distance from the treated vertebrae [11], locations near the thoracolumbar junction [11], advanced patient age [21],

Table 1 Results of univariate Cox proportional hazards regression analysis between patients with and without refracture of cemented vertebra

Variable	Total ($N = 81$)	Refracture ($N = 46$)	No refracture ($N = 43$)	p value	ORs	95% CI
Patient characteristics						
Age (years)	74.3 ± 7.2	75.0 ± 6.8	73.3 ± 7.6	0.099	1.039	0.993–1.086
Gender (female)	73 (90)	41 (89)	32 (91)	0.292	0.604	0.237–1.543
Body weight (kg)	56.6 ± 12.1	56.2 ± 12.4	57.1 ± 12.0	0.620	1.007	0.980–1.034
Body height (cm)	153.9 ± 8.5	152.0 ± 8.4	154.2 ± 8.3	0.391	0.982	0.942–1.024
Lumbar spine BMD (g/cm^2)	0.68 ± 0.15	0.67 ± 0.22	0.69 ± 0.17	0.418	0.864	0.811–0.947
Imaging and technical characteristics						
Treated vertebral level (T10–L2)	54 (67)	37 (80)	17 (49)	0.075	0.424	0.204–0.883
Gas–containing vertebra pre–Tx (yes)	31 (38)	23 (50)	8 (23)	0.022*	0.585	0.325–1.054
Patterns of vertebral fractures (wedge)	30 (37)	19 (41)	11 (26)	0.013*	2.153	1.174–3.946
Cement injected (mL)	5.49 ± 2.6	5.70 ± 2.6	5.21 ± 2.6	0.528	1.036	0.929–1.154
Cement leakage into disc	17 (21)	8 (17)	9 (26)	0.365	1.644	0.561-4.818
Standardized SI of the injured vertebrae						
T1-weighted	0.60 ± 0.21	0.56 ± 0.19	0.65 ± 0.22	0.150	0.313	0.064–1.525
T2-weighted	0.77 ± 0.27	0.70 ± 0.25	0.85 ± 0.28	0.009*	0.207	0.064–0.670
SI ratio of the injured vertebrae (FS C+)						
Well-enhanced zone	1.28 ± 0.24	1.31 ± 0.22	1.23 ± 0.26	0.002*	7.503	2.056–27.384
Poorly enhanced zone	0.59 ± 0.18	0.58 ± 0.14	0.61 ± 0.22	0.116	4.119	0.706–24.030
Volume ratio of the injury vertebrae (FS C+)						
Well-enhanced zone	0.62 ± 0.23	0.60 ± 0.21	0.64 ± 0.26	0.010*	0.168	0.043–0.655
Poorly enhanced zone	0.38 ± 0.23	0.40 ± 0.21	0.36 ± 0.26	0.010*	5.944	1.526–23.149

BMD bone mineral density, *Tx* treatment, *SI* signal intensity, *FS C+* Gd-DTPA-enhanced fat-suppression, *N* number of case, *OR* odd ratio, *CI* confidence interval

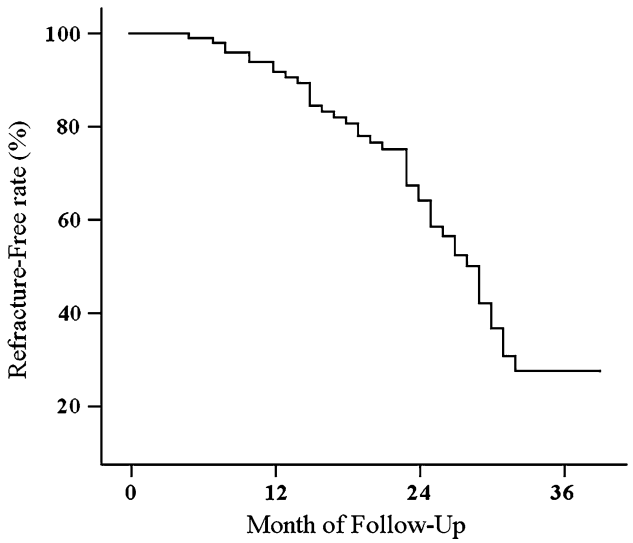

Fig. 2 The refracture-free rate of cemented vertebrae at different time intervals after vertebroplasty

small vertebrae before treatment [22], and treatment of multiple vertebrae [21]. Greater height restoration, with an existing intraosseous cleft, was also considered to be a potential risk factor for refracture of cemented vertebrae [9]. In this study, we also found a higher incidence of intraosseous clefts in the refracture group. The prevalence of a cleft sign ranges from 0.85% on radiographs of patients with VCFs [23] to 7% on CT images [24]. In selected patients with only osteoporotic VCFs, a frequency of 10–53% is possible [25]. The incidence is higher when MRI is used [25, 26], and in this study was 38%, since MRI is more sensitive for fluid-filled cleft detection. In non-treated injured vertebrae, the present of an intraosseous cleft and greater non-contrast area of the injured vertebra have also been found to cause progression of collapse [27, 28]. Our result is comparable to literature reports that indicate that an intraosseous cleft can be evaluated efficaciously by preoperative MRI to predict further cemented vertebral collapse [27, 28].

The typical MR finding in acute compression fracture is hypointensity on T1-weighted images, hypointensity or heterogeneous intensity on T2-weighted images, and hyperintensity on fat-suppressed T2-weighted images or on short-inversion time-inversion recovery images [16]. Diffusion weighted images show increases in water mobility in the bone marrow due to an expansion of the interstitial space after injury [29]. More severe injury may lead to obvious increase in interstitial space, which causes a

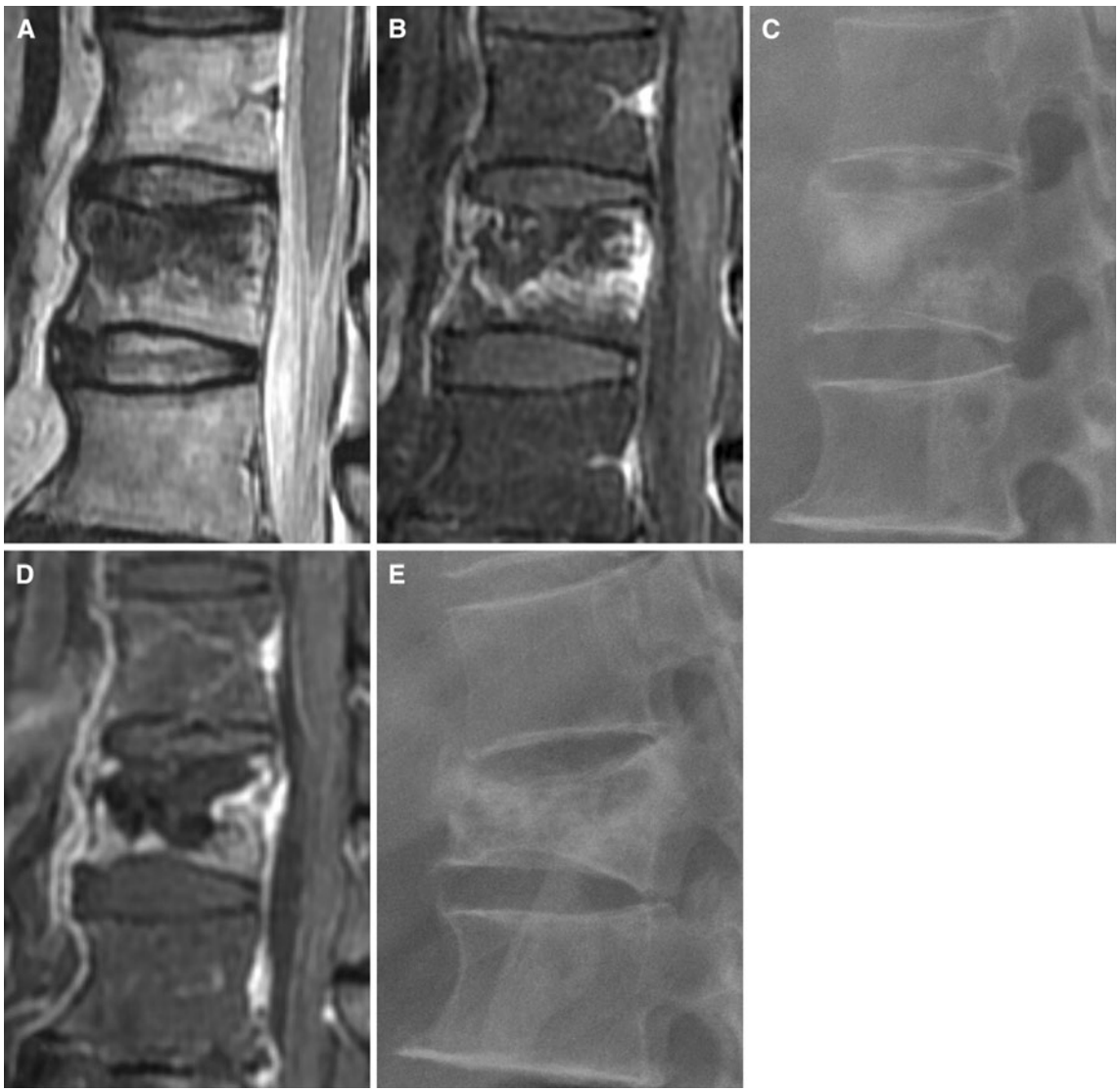

Fig. 3 Images of a 62-year-old man. T2-weighted images (**a**) and T1-weighted-enhanced fat-suppression images (**b**) show a large, poorly enhanced zone in the L1 vertebra (*arrow*). **c** Plain radiographic image immediately after vertebroplasty. (**d**) Follow-up MRI 1 month after the procedure showed a recurrent fracture with increased enhancement of the inferior-posterior vertebra. **e** Further collapse of the treated vertebra was found 6 months after vertebroplasty

greater decrease in SI on T1- and T2-weighted images (Table 1). If the fracture is severe, failure to achieve union and pseudoarthritis occurs at the site of the fractured endplate [28]. Intravertebral cavities filled with fluid, gas, or necrotic tissue [30] cause a further drop in SI on T1- and T2-weighted images. Our study demonstrates that any 1% decrease in standardized SI on T2-weighted images of the injured vertebra will increase the refracture rate by 0.76%.

In spinal MRIs, the area of contrast enhancement may be granulation tissue, fibrosis, inflammation, and/or edema, indicating an unhealed fracture [31]. In our patients, abnormal enhancement of bone marrow on MRIs can be seen up to 12 weeks after the initial fracture event. The higher degree of enhancement in these areas reflects a more acute process and more trabecular injury. Severely osteoporotic vertebral bodies are more susceptible to refracture. Non-healing or refracture results in progressive volume loss during the healing process [32]. The unenhanced area may be fluid, gas, necrosis, or avascular bone marrow. The poor enhancement in these areas suggests that the contents of the vertebrae are non-viable. Although not in the final refracture prediction model during follow-up, there was a greater SI increase in the well-enhanced zone and a greater SI decrease in the poorly enhanced zone in the refracture group, indicating diminished bone marrow integrity (Table 1).

Aside from an effective histopathological evaluation, enhanced MRI could be used for poorer bone marrow

quantification. We demonstrated that a 1% increase in the poorly enhanced volume ratio will increase the refracture rate by 3.8%. In fractures with an unfavorable prognosis, the ischemic area is usually wider, and restoration of vascularity is difficult [33]. By using dynamic MRI, Kanchiku et al. [27] demonstrated that the greater the noncontrast area in the injured vertebrae, the greater the subsequent progression of vertebral collapse. For ROI measurement, they used mid-sagittal MRI while we used five central sagittal views that covered a major portion of the vertebrae. In many instances, the vertebral injury involves only lateral part of the endplate and may not be fully represented in mid-sagittal images. Although it is possible to underestimate the unenhanced volume ratio by using mid-sagittal MRI, a problem is that delayed images may overestimate the enhanced part due to delays in contrast extravasation into the avascular zone, which would not increase SI during early dynamic imaging.

Cement distribution patterns also correlated well with bone marrow integrity, which may influence the prognosis of cemented vertebrae. In a fat-suppressed contrast-enhanced MRI study [15], a solid distribution pattern of injected cement was observed in all unenhanced areas, while outside the unenhanced area a solid pattern was not observed. Technically, the unenhanced areas, which are usually located anterior-superiorly, tend to be filled easily during the procedure. The minimal resistance from the cleft was prone to leaving the posterior enhanced area unfilled. The higher the unenhanced volume ratio of injured vertebrae, the more intravertebral space would be replaced by rigid cement. This suggests that crushing of the unfilled, small, enhanced part of the injured vertebrae by the cemented portion is inevitable (Fig. 3).

There are several limitations in this study. The refractures were identified on the basis of radiographic findings during follow-up after varying time periods. We were not able to obtain all the pain relief, relapse, and neurological data for all patients during their follow-up and could not draw conclusions regarding clinical symptom and AVH loss. The actual time interval between the occurrence of back pain and performing the MRI study was not available at data collection. The time effort required for quantification of the SI and volume parameters in the preoperative MRI is unknown. Patients with multiple or repeat vertebroplasty were not enrolled in this study. The influence between cemented–cemented vertebrae and cemented–normal-cemented vertebrae were not investigated.

Conclusion

Although vertebroplasty can initially stabilize injured vertebrae, further collapse of the cemented vertebrae occurred rapidly during follow-up. In this study, significant pre-procedure MRI-based predictors of increased risk for cemented vertebral refracture have been identified.

Acknowledgments This work was partly supported by grants from Chang Gung Memorial Hospital (Chang Gung Medical Research Project; CMRPG860101 to C.-C. Lui).

Conflict of interest statement None.

References

1. Jensen ME, Evans AJ, Mathis JM, Kallmes DF, Cloft HJ, Dion JE (1997) Percutaneous polymethylmethacrylate vertebroplasty in the treatment of osteoporotic vertebral body compression fractures: technical aspects. AJNR Am J Neuroradiol 18:1897–1904
2. Buchbinder R, Osborne RH, Ebeling PR, Wark JD, Mitchell P, Wriedt C, Graves S, Staples MP, Murphy B (2009) A randomized trial of vertebroplasty for painful osteoporotic vertebral fractures. N Engl J Med 361:557–568
3. Kallmes DF, Comstock BA, Heagerty PJ, Turner JA, Wilson DJ, Diamond TH, Edwards R, Gray LA, Stout L, Owen S, Hollingworth W, Ghdoke B, Annesley-Williams DJ, Ralston SH, Jarvik JG (2009) A randomized trial of vertebroplasty for osteoporotic spinal fractures. N Engl J Med 361:569–579
4. Belkoff SM, Mathis JM, Jasper LE, Deramond H (2001) The biomechanics of vertebroplasty. The effect of cement volume on mechanical behavior. Spine 26:1537–1541
5. Hiwatashi A, Moritani T, Numaguchi Y, Westesson PL (2003) Increase in vertebral body height after vertebroplasty. AJNR Am J Neuroradiol 24:185–189
6. Teng MM, Wei CJ, Wei LC, Luo CB, Lirng JF, Chang FC, Liu CL, Chang CY (2003) Kyphosis correction and height restoration effects of percutaneous vertebroplasty. AJNR Am J Neuroradiol 24:1893–1900
7. Garfin SR, Yuan HA, Reiley MA (2001) New technologies in spine: kyphoplasty and vertebroplasty for the treatment of painful osteoporotic compression fractures. Spine 26:1511–1515
8. Trout AT, Kallmes DF, Lane JI, Layton KF, Marx WF (2006) Subsequent vertebral fractures after vertebroplasty: association with intraosseous clefts. AJNR Am J Neuroradiol 27:1586–1591
9. Lin WC, Lee YC, Lee CH, Kuo YL, Cheng YF, Lui CC, Cheng TT (2008) Refractures in cemented vertebrae after percutaneous vertebroplasty: a retrospective analysis. Eur Spine J 17:592–599
10. Lin WC, Cheng TT, Lee YC, Wang TN, Cheng YF, Lui CC, Yu CY (2008) New vertebral osteoporotic compression fractures after percutaneous vertebroplasty: retrospective analysis of risk factors. J Vasc Interv Radiol 19:225–231
11. Kim SH, Kang HS, Choi JA, Ahn JM (2004) Risk factors of new compression fractures in adjacent vertebrae after percutaneous vertebroplasty. Acta Radiol 45:440–445
12. Do HM (2000) Magnetic resonance imaging in the evaluation of patients for percutaneous vertebroplasty. Top Magn Reson Imaging 11:235–244
13. Stallmeyer MJ, Zoarski GH, Obuchowski AM (2003) Optimizing patient selection in percutaneous vertebroplasty. J Vasc Interv Radiol 14:683–696
14. Dansie DM, Luetmer PH, Lane JI, Thielen KR, Wald JT, Kallmes DF (2005) MRI findings after successful vertebroplasty. AJNR Am J Neuroradiol 26:1595–1600
15. Oka M, Matsusako M, Kobayashi N, Uemura A, Numaguchi Y (2005) Intravertebral cleft sign on fat-suppressed contrast-enhanced

MR: correlation with cement distribution pattern on percutaneous vertebroplasty. Acad Radiol 12:992–999
16. Tanigawa N, Komemushi A, Kariya S, Kojima H, Shomura Y, Ikeda K, Omura N, Murakami T, Sawada S (2006) Percutaneous vertebroplasty: relationship between vertebral body bone marrow edema pattern on MR images and initial clinical response. Radiology 239:195–200
17. Cotten A, Boutry N, Cortet B, Assaker R, Demondion X, Leblond D, Chastanet P, Duquesnoy B, Deramond H (1998) Percutaneous vertebroplasty: state of the art. Radiographics 18:311–320 (discussion 320–313)
18. Gaughen JR Jr, Jensen ME, Schweickert PA, Marx WF, Kallmes DF (2002) The therapeutic benefit of repeat percutaneous vertebroplasty at previously treated vertebral levels. AJNR Am J Neuroradiol 23:1657–1661
19. Lin CC, Chen IH, Yu TC, Chen A, Yen PS (2007) New symptomatic compression fracture after percutaneous vertebroplasty at the thoracolumbar junction. AJNR Am J Neuroradiol 28:1042–1045
20. Ahn Y, Lee JH, Lee HY, Lee SH, Keem SH (2008) Predictive factors for subsequent vertebral fracture after percutaneous vertebroplasty. J Neurosurg Spine 9:129–136
21. Lee WS, Sung KH, Jeong HT, Sung YS, Hyun YI, Choi JY, Lee KS, Ok CS, Choi YW (2006) Risk factors of developing new symptomatic vertebral compression fractures after percutaneous vertebroplasty in osteoporotic patients. Eur Spine J 15:1777–1783
22. Hiwatashi A, Yoshiura T, Yamashita K, Kamano H, Dashjamts T, Honda H (2009) Subsequent fracture after percutaneous vertebroplasty can be predicted on preoperative multidetector row CT. AJNR Am J Neuroradiol 30:1830–1834
23. Kumpan W, Salomonowitz E, Seidl G, Wittich GR (1986) The intravertebral vacuum phenomenon. Skelet Radiol 15:444–447
24. Stäbler A, Schneider P, Link TM, Schöps P, Springer OS, Dürr HR, Reiser M (1999) Intravertebral vacuum phenomenon following fractures: CT study on frequency and etiology. J Comput Assist Tomogr 23:976–980
25. Lane JI, Maus TP, Wald JT, Thielen KR, Bobra S, Luetmer PH (2002) Intravertebral clefts opacified during vertebroplasty: pathogenesis, technical implications, and prognostic significance. AJNR Am J Neuroradiol 23:1642–1646
26. Peh WC, Gelbart MS, Gilula LA, Peck DD (2003) Percutaneous vertebroplasty: treatment of painful vertebral compression fractures with intraosseous vacuum phenomena. AJR Am J Roentgenol 180:1411–1417
27. Kanchiku T, Taguchi T, Toyoda K, Fujii K, Kawai S (2003) Dynamic contrast-enhanced magnetic resonance imaging of osteoporotic vertebral fracture. Spine 28:2522–2526 (discussion 2522)
28. Naul LG, Peet GJ, Maupin WB (1989) Avascular necrosis of the vertebral body: MR imaging. Radiology 172:219–222
29. Baur A, Stäbler A, Brüning R, Bartl R, Krödel A, Reiser M, Deimling M (1998) Diffusion-weighted MR imaging of bone marrow: differentiation of benign versus pathologic compression fractures. Radiology 207:349–356
30. Ito Y, Hasegawa Y, Toda K, Nakahara S (2002) Pathogenesis and diagnosis of delayed vertebral collapse resulting from osteoporotic spinal fracture. Spine J 2:101–106
31. Uemura A, Kobayashi N, Numaguchi Y, Fuwa S, Saida Y (2007) Preprocedural MR imaging for percutaneous vertebroplasty: special interest in contrast enhancement. Radiat Med 25:325–328
32. Diamond TH, Clark WA, Kumar SV (2007) Histomorphometric analysis of fracture healing cascade in acute osteoporotic vertebral body fractures. Bone 40:775–780
33. Cho T, Matsuda M, Sakurai M (1996) MRI findings on healing process of vertebral fracture in osteoporosis. J Orthop Sci 1:16–33